New High-Throughput Screening Protease Assay Based upon Supramolecular Self-assembly

Zhijun Zhou,[†] Yanli Tang,[†] David G. Whitten,*[,†] and Komandoor E. Achyuthan*[,‡]

Department of Chemical and Nuclear Engineering, The University of New Mexico, Albuquerque, New Mexico 87131, and Biosensors and Nanomaterials Department, Sandia National Laboratories, Albuquerque, New Mexico 87185

ABSTRACT We previously demonstrated that the supramolecular self-assembly of cyanines could be useful for developing fluorescent enzymatic assays. We took that concept a step further by synthesizing a covalent adduct of the tetrapeptide Asp−Glu−Val−Asp (DEVD) and a cyanine (DEVD−cyanine). The DEVD−cyanine due to its canonical sequence was recognized and hydrolyzed by the proteases, Caspase-3 and -7 in 96- or 384-microwell plate reactions. The catalytically liberated cyanine self-assembled upon scaffolds of carboxymethylamylose (CMA), carboxymethylcellulose (CMC), or a mixture of CMA and CMC resulting in a J aggregate exhibiting bright fluorescence at a 470 nm emission wavelength (optimum signal/background using excitation wavelengths of 415−440 nm). The fluorescence intensity increased with enzyme and substrate concentrations or reaction time and exhibited classical saturation profiles of a rectangular hyperbola. Saturation of the reaction was at 30 U/mL (1 μg/mL) Caspase-3 and 250 μM DEVD−cyanine. The reaction kinetics was linear between 1 and 20 min and saturated at 60 min. The affinity constant (Km) for DEVD−cyanine was ~23 μM, similar to those of previously reported values for other DEVD substrates of Caspase-3. Maximal fluorescence emission was observed by using a mixture of CMA and CMC scaffolds at 65 and 35 μM, respectively. The reaction kinetics of Caspase-7 executed in a 384-well plate was similar to the reaction kinetics of Caspase-3 conducted in a 96-well plate. We believe that this is the first demonstration of a cyanine liberated from a covalent adduct due to protease action, leading to supramolecular self-assembly and the detection of protease activity.

KEYWORDS: DEVD tetrapeptide • cyanine • Caspase-3 • Caspase-7 • supramolecular • self-assembly • protease assay • high-throughput screening

INTRODUCTION

We previously reported that the nonfluorescent cyanine dye **1** (Figure 1) formed fluorescent "J aggregates" when the anionic biopolymer carboxymethylamylose (CMA) was added to solutions of **1** (1). While the glucose polymer amylose exists in nonaqueous media as a helical structure, the chemical addition of carboxyl groups renders the resultant CMA water-soluble. However, repulsions between nearby carboxyl groups destabilize the helical structure such that the CMA exists as an "interrupted helix" in water. The association of **1** with CMA is a cooperative self-assembly process, and the resulting host−guest complex is helical, involving strong association of **1** with each other and with CMA (1). The relatively broad absorption of **1** becomes red-shifted and sharpened upon association with CMA, and a sharp, strong fluorescence is observed (1). These spectral features along with strong, biphasic-induced circular dichroism were characteristic features of the "J aggregate" of achiral **1**, in which molecules of **1** were associated with each other in an end-on-end association (1, 2).

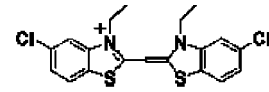

1

FIGURE 1. Structure of cyanine 1 with a molecular mass of 408.39. Cyanine 1 was modified to introduce a terminal amino group as shown in Figure 2. This amino group was used to tether the cyanine 2a covalently to the DEVD tetrapeptide.

Subsequent to our discovery of highly fluorescent J-aggregate formation between **1** and CMA, we developed bioassays based on cooperative self-assembly. We showed that the addition of CMA to nonfluorescent solutions of **1** resulted in a strongly fluorescent **1**−CMA complex, thus detecting the presence of the biopolymer. We also found that the salivary amylase enzyme unraveled the complex by hydrolyzing CMA and leading to a decrease in the fluorescence, producing a dose−response tracing that was an index of amylase activity (3, 4). Similar results were obtained with complexes that were formed between **1** and other anionic biopolymers such as carboxymethylcellulose (CMC) or hyaluronic acid (HA) (4, 5), and thus assays were developed for the hyaluronidase enzyme in order to detect HA hydrolysis (5). Finally, we found that the fluorescent complex

* Corresponding authors. Tel: 505-284-8979(K.E.A.), 505-277-5736(D.G.W.). Fax: 505-844-1198 (K.E.A.), 505-277-1292 (D.G.W.). E-mail: kachyut@sandia.gov (K.E.A.), whitten@langmuir.acs.org (D.G.W.).

Received for review October 1, 2008 and accepted December 8, 2008

[†] The University of New Mexico.

[‡] Sandia National Laboratories.

DOI: 10.1021/am800091h

Published on Web 01/07/2009

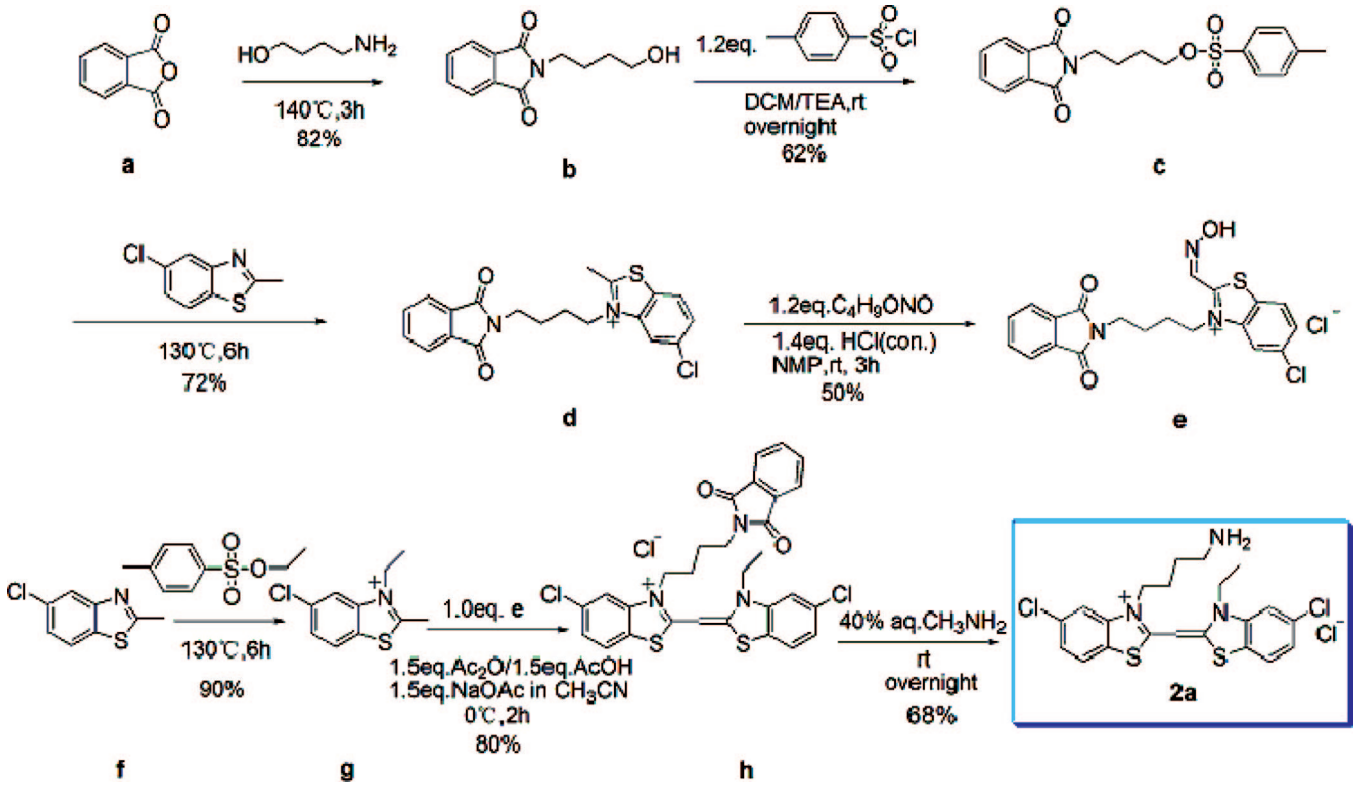

FIGURE 2. Synthetic scheme for cyanine 2a. The synthetic details are described in the Materials and Methods section of the paper.

between **1** and CMA was quenched by a cationic cyanine absorbing at longer wavelengths than the **1**−CMA J-aggregate complex and that the fluorescence quenching resulted in the sensitization of the quencher fluorescence (3). We also reported that **1** formed fluorescent J aggregates with nucleic acids, leading to a sensitive detection scheme for several different nucleic acid (DNA and RNA) scaffolds (6).

We took these concepts to a higher level by focusing upon the development of novel biosensing approaches based upon the release of the cyanine chromophore from a covalent adduct due to protease activity and thus demonstrating a new approach to sensing that extended the scope of the biopolymer−dye J-aggregate formation. The present work involved studies with an unsymmetrical cyanine (**2a**) that was synthesized according to a multistep procedure (Figure 2). The synthetic sequence affords a general method for preparing unsymmetrical cyanine dyes that can be coupled to biopolymers or oligomeric short peptides (as shown in Figure 3). Such covalent conjugates can be useful in the design of enzyme assays, such as, for example, the proteases like Caspases that are involved in apoptosis (or programmed cell death) (7−10) and therefore targets for drug discovery (11).

MATERIALS AND METHODS

Caspase-3 and -7 were purchased from Sigma-Aldrich (St. Louis, MO) either as part of a "combo kit" also containing Caspase-2 or as individual reagents from Sigma-Aldrich. The certificates of analyses received from the vendor for the specific lots of enzymes purchased gave the following definitions for the specific activities. (a) Caspase-3 and -7 ("combo kit"): one unit will cleave 1 nmol of the caspase substrate DEVD−pNA (*N*-acetyl-DEVD-*p*-nitroanilide) per 1 h at pH 7.2 at 37 °C. (b) Caspase-3 and -7 (individual reagent): one unit will hydrolyze 1.0 nmol of Ac-DEVD-AFC [*N*-acetyl-DEVD-7-amino-4-(trifluoromethyl)coumarin] per 1 min at pH 7.5 and 25 °C. The enzymes were stored in small aliquots at −80 °C until use. Enzyme aliquots were discarded after a single use and not subjected to more than a single freeze−thaw cycle. The carbohydrate scaffolds carboxymethylcellulose (CMC) and carboxymethylamylose (CMA) were also purchased from Sigma-Aldrich, dissolved in water as 1 and 2 mM solutions, respectively, and stored refrigerated. The protected DEVD synthetic peptide (except for the carboxy-terminal carboxyl group being free) was purchased from Bachem BioScience (King of Prussia, PA). The substrate DEVD−cyanine was synthesized and purified as described below. The substrate was dissolved in methanol as a 4 mM stock solution and stored refrigerated. The assay buffer consisted of 20 mM sodium phosphate, pH 7.5, supplemented with 100 mM sodium chloride, 0.1% 3-[(3-cholamidopropyl)-dimethylammonio]-1-propanesulfonate detergent, 10% glycerol, and 2 mM ethylenediaminetetraacetic acid. Just prior to use, freshly made dithiothreitol was added to the buffer at a concentration of 5 mM. Enzymatic reactions were carried out using 96- or 384-well white microplates (Optiplate, Perkin-Elmer, Waltham, MA). Both the enzyme and the substrate were diluted in the above buffer just prior to use.

DEVD−Cyanine Substrate Synthesis. The synthesis of the unsymmetrical cyanine **2a** was accomplished through a multistep scheme outlined in Figure 2 and is generally useful for preparing cyanines of similar structure for covalent attachment. The details for the synthesis are described below.

Synthesis of **b**: This was prepared by following the procedure described in the literature (12).

Synthesis of **c**: To a solution of **b** (200 mg, 0.91 mmol) in 2 mL of dichloromethane, cooled to 0 °C for 5 min, were added 4-toluenesulfonyl chloride (208 mg, 1.09 mmol) and triethylamine (184 mg, 0.25 mL, 1.82 mmol) under N_2. The solution was allowed to warm to room temperature and kept stirring overnight. The product was extracted by ethyl acetate, washed

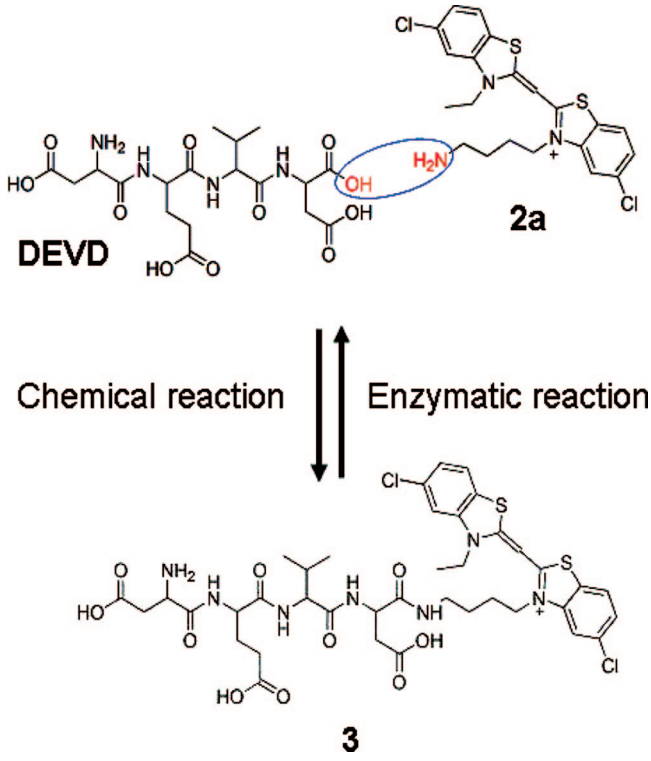

FIGURE 3. Schematics of DEVD−cyanine 3 and hydrolysis by Caspase-3 and -7. This cartoon depicts the chemical coupling strategy of the deprotected DEVD tetrapeptide to aminocyanine 2a resulting in 3 (downward-pointing arrow). The enzymatic reaction (upward-pointing arrow) shows the hydrolysis of 3 through Caspase-3 and -7 proteolysis. The amino and carboxyl groups involved in the chemical and enzymatic reactions are circled. The schematic *does not* indicate any type of equilibrium existing between the chemical coupling reaction and the enzymatic reaction.

by 5 mL of H_2O, then washed by 2 × 5 mL of a saturated sodium chloride solution, and dried by anhydrous $MgSO_4$. The product was purified by silica gel flash chromatography with a ratio of 2:1 hexane/ethyl acetate to provide 211 mg of a white solid. Yield: 62%. ^{1}H NMR (500 MHz, $CDCl_3$): δ 7.835 (dd, $J_1 = 3$ Hz, $J_2 = 5.5$ Hz, 2H), 7.792 (d, $J = 8$ Hz, 2H), 7.724 (dd, $J_1 = 3$ Hz, $J_2 = 5.5$ Hz, 2H), 7.342 (d, $J = 8$ Hz, 2H), 4.069 (t, $J = 6$ Hz, 2H), 3.661 (t, $J = 6.5$ Hz, 2H), 2.436 (s, 3H), 1.707 (m, 2H), 1.317 (m, 2H).

Synthesis of **d**: Compound **c** (1.662 g, 4.45 mmol) was added into a 25 mL ground-glass flask, followed by 5-chloro-2-methylbenzo[*d*]thiazole (0.82 g, 4.45 mmol). The reaction mixture was heated to 130 °C slowly under a N_2 atmosphere and allowed to stir for 6 h. It was then cooled to room temperature, and a solid was formed. Ethyl ether (5 mL) was added into the resulting mixture, which was stirred for 10 min and then filtered to provide a slightly green powder. The product was purified by inverse silica gel chromatography to give 1.78 g of a white solid product. Yield: 72%. ^{1}H NMR (500 MHz, $CDCl_3$): δ 8.263 (d, $J = 8.5$ Hz, 1H), 7.851 (s, 1H), 7.842 (dd, $J_1 = 3$ Hz, $J_2 = 5$ Hz, 2H), 7.748 (dd, $J_1 = 3$ Hz, $J_2 = 5$ Hz, 2H), 7.635 (d, $J = 8.5$ Hz, 1H), 7.594 (d, $J = 7.5$ Hz, 2H), 7.058 (d, $J = 7.5$ Hz, 2H), 4.927 (t, $J = 7.5$ Hz, 2H), 3.407 (s, 3H), 2.298 (s, 3H), 1.977 (m, 2H), 1.417 (t, $J = 8$ Hz, 2H), 1.111 (m, 2H).

Synthesis of **e**: A solution of **d** (200 mg, 0.371 mmol) in 3 mL of 1-methyl-2-pyrrolidinone was cooled to 0 °C, and to this solution was then added a 37% hydrochloride solution (43 μL, 0.519 mmol) and C_4H_9ONO (0.05 mL, 0.445 mmol). The mixture was stirred for 3 h at room temperature, and then 3 mL of dichloromethane was added into the mixture to give a precipitate. The white solid was provided after filtration, washed with dichloromethane and ethyl ether, and then air-dried to give 84 mg of product. Yield: 50%. The product was directly used for the next step without further purification. ^{1}H NMR (500 MHz, DMSO-d_6): δ 8.411 (s, 1H), 7.825 (s, 1H), 7.634 (d, $J = 9$ Hz, 0.75H), 7.583 (d, $J = 8.5$ Hz, 0.25H), 7.063 (d, $J = 8.5$ Hz, 1H), 7.030 (m, 4H), 4.082 (t, $J = 7.5$ Hz, 1.5H), 4.003 (t, $J = 8$ Hz, 0.5H), 2.806 (t, $J = 6.5$ Hz, 2H), 1.044 (m, 4H).

Synthesis of **g**: This was prepared by following the procedure described in the synthesis of **d**. Yield: 90%. ^{1}H NMR (500 MHz, $CDCl_3$): δ 8.093 (d, $J = 8.5$ Hz, 1H), 7.848 (s, 1H), 7.633 (d, $J = 8.5$ Hz, 1H), 7.591 (d, $J = 8$ Hz, 2H), 7.042 (d, $J = 8$ Hz, 2H), 4.900 (q, $J = 7.5$ Hz, 2H), 3.377 (s, 3H), 2.290 (s, 3H), 1.575 (t, $J = 7$ Hz, 3H).

Synthesis of **h**: A solution of **e** (100 mg, 0.222 mmol) in 1.5 mL of acetonitrile was cooled to 0 °C, and then **g** (85.2 mg, 0.222 mmol), acetic anhydride (34 mg, 0.333 mmol), acetic acid (20 mg, 0.333 mmol), and sodium acetate (27 mg, 0.333 mmol) were added into the mixture. The reaction was stirred at 0 °C for 2 h. The resulting suspension was filtered and washed with dichloromethane and a small amount of ice water to give a yellow powder. The product was purified by inverse silica gel chromatography to give 110 mg of a yellow solid. ^{1}H NMR (500 MHz, DMSO-d_6): δ 8.240 (d, $J = 8.5$ Hz, 1H), 8.115 (s, 1H), 8.067 (s, 1H), 7.801 (d, $J = 8.5$ Hz, 1H), 7.779 (d, $J = 7.5$ Hz, 1H), 7.570 (d, $J = 7.5$ Hz, 1H), 7.741 (d, $J = 8.0$ Hz, 2H), 7.103 (d, $J = 8.0$ Hz, 2H), 6.653 (s, 1H), 4,650 (q, $J = 8$ Hz, 2H), 2.825 (t, $J = 7.5$ Hz, 2H), 1.911 (m, 2H), 1.742 (m, 2H), 1.378 (t, $J = 8.4$ Hz, 2H), 1,265 (t, $J = 8$ Hz, 3H).

Synthesis of **2a**: Solid **h** (540 mg, 0.875 mmol) was added into 30 mL of a 40% CH_3NH_2 aqueous solution, which was then allowed to stir overnight at room temperature. The solvent and CH_3NH_2 were removed by rotary evaporation to give a yellow solid. The product was purified by inverse-phase silica gel chromatography to give 290 mg of a yellow solid. ^{1}H NMR (500 MHz, DMSO-d_6): δ 8.271 (d, $J = 8.5$ Hz, 1H), 8.124 (s, 1H), 7.594 (d, $J = 8.5$ Hz, 1H), 7.465 (d, $J = 7.5$ Hz, 1H), 7.101 (d, $J = 7.5$ Hz, 1H), 6.72 (s, 1H), 5.74 (s, 1H), 4.701 (q, $J = 8$ Hz, 2H), 2.788 (t, $J = 7.5$ Hz, 2H), 2.273 (s, 2H), 1.822 (m, 2H), 1.645 (m, 2H), 1.371 (t, $J = 8.4$ Hz, 2H), 1.225 (t, $J = 8$ Hz, 3H). MS (ESI). Calcd: *m*/*z* 450.06. Obsd: *m*/*z* 450.0627.

The synthesis of the DEVD−cyanine covalent conjugate was carried out as described below.

Synthesis of protected DEVD−cyanine: A solution of protected DEVD (100 mg, 0.134 mmol) in 2 mL of *N*,*N*-dimethylformamide was cooled to 0 °C, and then hydroxybenzotriazole (27.2 mg, 0.201 mmol) and diisopropylcarbodiimide (20.3 mg, 0.161 mmol) were added into the mixture. The resulting mixture was allowed to stir for 10 min, followed by the addition of **2a** (65 mg, 0.134 mmol). This mixture was stirred overnight, and then the solvent was removed by vacuum evaporation with an oil pump to give a yellow solid. The product was purified by inverse-phase silica gel chromatography to provide 139 mg of product. Yield: 85%. ^{1}H NMR (500 MHz, DMSO-d_6): δ 8.258 (d, $J = 7.5$ Hz, 1H), 8.116 (s, 1H), 7.885 (m, 3H), 7.732 (m, 2H), 7.577 (d, $J = 8.5$ Hz, 1H), 7.468 (d, $J = 7.5$ Hz, 1H), 7.183 (d, $J = 7.5$ Hz, 1H), 7.101 (s, 1H), 6.713 (s, 1H), 5.293 (m, 2H), 4.698 (m, 2H), 4.344 (m, 4H), 2.622 (m, 6H), 2.154 (m, 4H), 1.585 (m, 2H), 1.408 (s, 36H), 1.208 (m, 4H), 1.058 (t, $J = 7$ Hz, 3H), 0.725 (d, $J = 6.5$ Hz, 6H). MS (ESI). Calcd: *m*/*z* 1176.47. Obsd: *m*/*z* 1176.4669.

Synthesis of DEVD−cyanine: A solution of protected DEVD−cyanine (100 mg, 0.085 mmol) in 1.8 mL of a CF_3COOH solution was cooled to 0 °C. To this solution was then added 0.1 mL of H_2O and 0.1 mL of triisopropylsilane (TIPS), and the resulting mixture was stirred overnight. The solvent was removed by vacuum evaporation to give a yellow oil. The product was further purified by inverse-phase silica gel chromatography to provide 77 mg of a yellow solid. Yield: 92%. ^{1}H NMR (500 MHz, DMSO-d_6): δ 8.558 (d, $J = 7.5$ Hz,

1H), 8.250 (s, 1H), 8.120 (m, 3H), 7.860 (d, $J = 8.5$ Hz, 2H), 7.573 (d, $J = 7.5$ Hz, 1H), 7.453 (d, $J = 7.5$ Hz, 1H), 7.077 (s, 1H), 6.700 (s, 1H), 4.677 (m, 3H), 4.380 (m, 1H), 3.645 (m, 4H), 3.116 (m, 5H), 2.351 (m, 2H), 2.275 (m, 2H), 1.878 (m, 2H), 1.445 (m, 4H), 1.222 (m, 3H), 0.969 (m, 6H). MS (ESI). Calcd: *m*/*z* 908.23. Obsd: *m*/*z* 908.0247.

Caspase Protease Assay. Reactions were carried out in 96- or 384-well white microplates. Both the enzyme and substrate were diluted using an assay buffer with the composition described in the Materials and Methods section of the paper (vide supra). Typically, 5 μL of the enzyme solution was mixed with 5 μL of the DEVD−cyanine substrate. The enzymatic hydrolysis of the substrate was carried out at 37 °C after tightly sealing the plate using commercial sealing tape (ImmunoWare Sealing Tape, Pierce, Rockford, IL) in order to minimize evaporative losses arising due to assay miniaturization. Reactions were terminated by dilution to a total volume of 280 μL (96-well plate reactions) or 95 μL (384-well plate reactions) using a mixture of methanol/water (20:80). Unless indicated otherwise, J aggregation of the liberated cyanine was initiated by the addition of 20 μL (96-well plate reactions) or 5 μL (384-well plate reactions) of a mixture of CMA and CMC scaffolds, such that the final concentrations of the twin scaffolds were approximately 65 μM CMA and 35 μM CMC. The final volume in each well was thus 300 μL (96-well plate reactions) or 100 μL (384-well plate reactions). The plates were then incubated at room temperature (~25 °C for 30 min) before taking fluorescence measurements. Control reactions to determine background fluorescence included reaction wells containing enzyme only, substrate only, or the reaction buffer without enzyme and substrate.

Fluorescence Measurements. Fluorescence measurements were taken using a Molecular Devices (Sunnyvale, CA) microplate reader. Samples were excited over the wavelength range of 415−440 nm, and the emission intensity was measured at 470 nm. In some experiments, both the excitation and emission wavelengths were varied in order to achieve optimal conditions for fluorescence detection of DEVD−cyanine cleavage by protease. Fluorescence emission was corrected for the small extent (typically <10% of maximal fluorescence from the J aggregate) of intrinsic light emission from the DEVD−cyanine intact substrate molecule. Microplate-based assays were designed, keeping the design principles described by us recently (13).

Data Analysis. All reactions were carried out in triplicate, and the values were calculated as average ± standard deviation for each determined parameter. *Kaleidagraph* software (version 4.03, Synergy software, Reading, PA) was used to generate the tracings shown for the various experiments. The control reaction giving the maximal background fluorescence was used to correct the signal arising from the complete enzymatic reaction. In these experiments, the low intrinsic fluorescence arising from DEVD−cyanine (minus the Caspase) was used for correction, and the resultant tracing was represented as relative fluorescence units (RFUs). Values are the average of triplicate measurements for each determined parameter. Where not visible, error bars are masked within the symbol. The limits of detection and quantitation were calculated as described previously (14). Data obtained from a study of the effects of the substrate concentration on the reaction velocity were transformed using the Eadie−Hofstee equation [$V/(V/S)$] using the software program *EnzymeKinetics Pro!* (version 2.36, SynexChem LLC, Fairfield, CA). This transformation allowed us to calculate the enzyme kinetic parameter Km. Km, sometimes called the Michaelis constant, involves the equilibrium between the formation of the enzyme−substrate (ES) complex as well as its breakdown into enzyme and products (E + P). While Km does not refer to the binding constant or binding strength of the substrate to the enzyme, it does encompass the affinity of the substrate for the enzyme as well as the rate at which the substrate bound to the enzyme is converted into product(s). A basic definition of Km is that it represents that concentration of a given substrate at which the enzyme-catalyzed reaction reaches half of the maximal velocity. Thus, Km = $V_{max}/2$. In other words, a high Km value denotes a substrate that is not efficiently converted into product because it requires a larger concentration of substrate to achieve half of the maximal velocity. Conversely, a low Km indicates a greater affinity of the substrate for the enzyme and a higher rate of substrate conversion into product. In certain experiments, the S/B ratio was used to evaluate the data.

RESULTS AND DISCUSSION

In the present study, a protected tetrapeptide containing the canonical sequence Asp−Glu−Val−Glu (DEVD) for specific recognition by Caspase-3 and -7 (7−10) was covalently linked to a modified unsymmetrical cyanine (**2a**; Figure 3). Compound **2a** was synthesized in good overall yield by the scheme outlined in Figure 2. The reactions used in this synthetic scheme can be generally useful for the synthesis of unsymmetrical cyanines for covalent attachment. Herein, **2a** was coupled using *N*-hydroxysuccinimide activation with a synthetic protected peptide (DEVD) at the unprotected carboxyl terminus to afford a protected tetrapeptide. The protected peptide was then deprotected in a one-step reaction with trifluoroacetic acid in dichloromethane to yield the DEVD−cyanine peptide **3**. The DEVD−cyanine peptide **3** was designed as a substrate for the proteases Caspase-3 and -7 (7−10).

The synthetic tetrapeptide **3** (DEVD−cyanine, shown as a deprotected peptide in Figure 3) was selected as a prototype for a wide array of biomolecules incorporating a sequence that is recognized by a specific enzyme and can subsequently be reacted to release a reporter molecule, in this case **2a**. The sequence recognized by Caspase-3 and -7 is a short tetrapeptide, DEVD (7−10). DEVD when linked to cyanine **2a** and then deprotected (**3**) is a dianion at neutral pH (Figure 3). As anticipated, **3** in an aqueous solution did not associate with CMA or CMC, and the appended cyanine was nonfluorescent both in aqueous media and in aqueous solutions in the presence of anionic biopolymers such as CMA or CMC. However, the dicationic cyanine **2a** (in neutral aqueous solutions) is released by the enzymatic cleavage of **3**. For hydrolysis of the DEVD−cyanine substrate, we purchased Caspase-3 and -7 from Sigma-Aldrich. The enzymatic reaction was carried out essentially as described by us previously (10). The "free" **2a** that was liberated by enzymatic hydrolysis readily self-assembles upon CMC or CMA scaffolds to form a fluorescent J aggregate and provides a sensitive assay of Caspase-3 and/or -7 to hydrolyze **3**.

There was an increase in fluorescence between 450 and 550 nm emission wavelengths as a function of the enzyme concentration when Caspase-3 was incubated with **3** and then either CMC or CMA was added postcatalysis (Figure 4A). The excitation wavelength was varied from 415 to 440 nm in 5 nm intervals. For each excitation wavelength, fluorescence from the J aggregate of the released cyanine **2a** self-assembling upon the scaffold was measured over an emission wavelength range of 410−550 nm (Figure 4A). It is important to note that in these experiments the intact

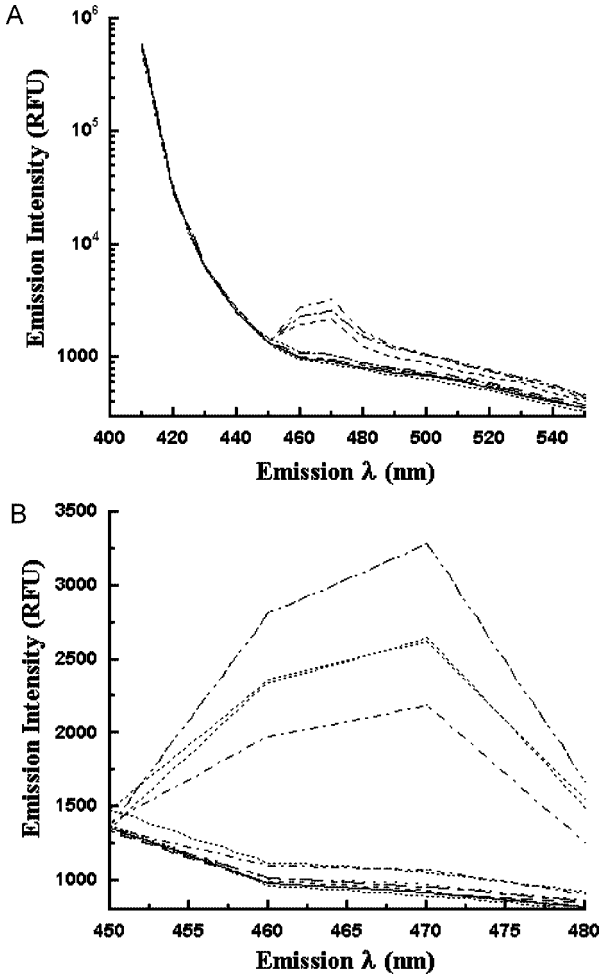

FIGURE 4. (A) Emission wavelength scan of the reactions of DEVD−cyanine with increasing concentrations of Caspase-3. Only a representative example of the scan for $\lambda_{ex} = 400$ nm is shown in this figure. The various tracings represent progressively increasing concentrations of Caspase-3 (0, 1, 2.5, 5, 10, 15, 30, and 60 U/mL) utilized to catalyze the hydrolysis of the DEVD−cyanine substrate. Fluorescence emission was scanned over the indicated wavelength range in 2 nm intervals. (B) Exploded view of the desired range of fluorescence emission wavelengths between 450 and 480 nm. This figure is intended to show clearly the Caspase-3 concentration-dependent increase in the peak fluorescence at 470 nm. The Caspase-3 concentrations used and the scan intervals were the same as those listed in part A.

DEVD−cyanine substrate did not self-assemble upon the carbohydrate scaffolds. Consequently, there were only very low levels of light emission from the substrate in the absence of the Caspase-3 enzyme. We considered this as background and either corrected for it (ΔRFU) or used the background emission values to calculate the ratio of signal to background (S/B). It was only the cleaved product, the "free" cyanine, that was capable of efficient self-assembly upon the twin carbohydrate scaffolds (Figures 4 and 5). A clear increase in the fluorescence emission was particularly noticeable between wavelengths of 460 and 470 nn (Figure 4B). The maximum fluorescence was detected at a peak emission wavelength of 470 nm (Figure 4B). A chart of the S/B values showed that the excitation wavelengths between 420 and 440 nm gave optimum fluorescence emission without serious signal degradation due to the rising blank fluorescence (Figure 5). At excitation wavelength values

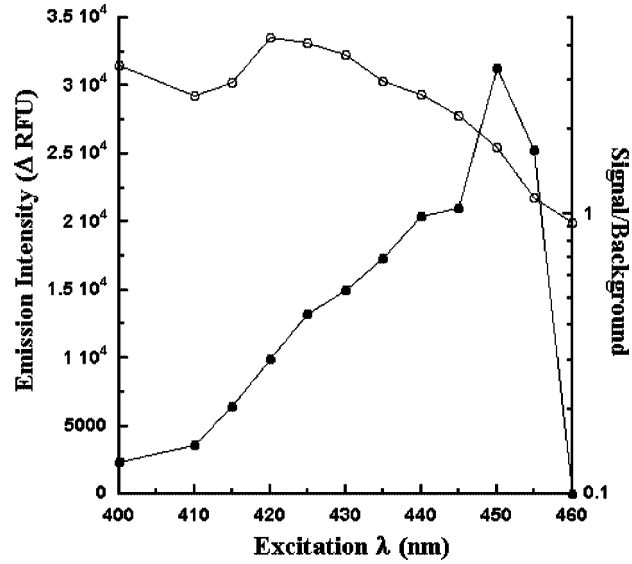

FIGURE 5. Effect of the excitation wavelength on the fluorescence emission intensity at 470 nm and the S/B of Caspase-3 catalysis. Caspase-3 (30 U/mL) was used to catalyze the hydrolytic reactions of DEVD−cyanine. The open circles represent the S/B values, and the closed circles represent the fluorescence emission intensity corrected for background fluorescence (ΔRFU) from DEVD−cyanine in the absence of enzyme. The reaction samples were scanned over excitation wavelengths of 400−460 nm in 5 nm intervals.

above or below this threshold, S/B declined, even though the fluorescence signal strength continued to increase up 450 nm excitation wavelength and decline thereafter (Figure 5). However, we considered the deterioration in the S/B values at excitation wavelengths of 450 nm or higher as unacceptable in the delivery of a robust protease assay. Therefore, in all further experiments, the emission wavelength was fixed at 470 nm and the fluorescence from the reaction samples was measured by excitation of the samples between the wavelengths of 420 and 445 nm at 5 nm intervals. It is also important to note that the results shown in Figures 4 and 5 were conducted under assay conditions that had not yet been sufficiently optimized. There were also some differences in the magnitude of the separation between the tracings of the various concentrations of Caspase-3 enzyme depending upon the excitation wavelengths (Figure 4). These experiments were done for the sole purpose of establishing the optimal excitation and emission wavelengths. This might also explain the differences in the tracings of Figure 4 compared to Figure 6 that are discussed elsewhere in this paper.

The J aggregation may be perturbed by enzymatic reaction components such as buffer salts, sodium chloride, detergent, or thiol reagent (2, 6). We therefore investigated the effects of well volume upon the fluorescence emission intensity and S/B. We found that diluting the well volume 30-fold (96-well reactions) or 10-fold (384-well reactions) using a methanol/water mixture before adding CMA and CMC facilitated a more optimal self-assembly of the liberated cyanine upon the carbohydrate scaffolds. Preliminary experiments showed that for 96-well plate reactions a final well volume of 150−300 μL yielded maximum fluorescence emission and higher S/B values. The decline in the fluores-

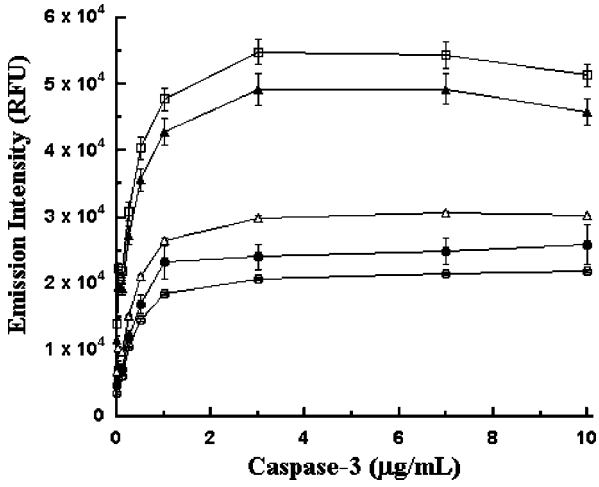

FIGURE 6. Caspase-3 dose−response chart. Increasing and indicated concentrations of Caspase-3 enzyme were reacted with 250 μM DEVD−cyanine substrate at 37 °C for 90 min. The various tracings represent increasing fluorescence emission intensities observed at 470 nm emission wavelength and several different excitation wavelengths as follows: open circles, 420 nm; closed circles, 425 nm; open triangles, 430 nm; closed triangles, 435 nm; open squares, 440 nm. All other conditions are as described in the Materials and Methods section of the paper.

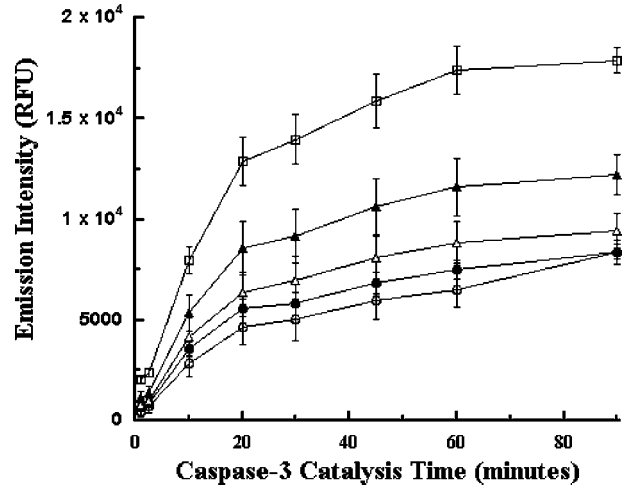

FIGURE 7. Caspase-3 reaction kinetics. This chart shows the reaction progress curves for Caspase-3-catalyzed hydrolysis of the DEVD−cyanine substrate. Caspase-3 (0.2 μg/mL) was reacted with 250 μM substrate at 37 °C for the indicated reaction time periods. All other conditions were as described in the legend of Figure 6.

cence intensity and S/B values observed with well volumes flanking these limits (50 and 100 μL and 350 and 400 μL, respectively) could be due to interference from assay buffer components at lower volumes and suboptimal scaffold concentrations due to increased dilution at higher volumes. At the lower well volumes of 50 and 100 μL, there might also be an "inner filter effect" arising from the higher scaffold concentrations and resulting in a fluorescence quench (5).

Two different batches and lots of Caspase-3 were tested in order to confirm the hydrolysis of the DEVD−cyanine **3** substrate in our new high-throughput screening (HTS) assay system for proteases. The results were overall similar to those of proteolytic digestion of the substrate taking place linearly between Caspase-3 concentrations of 0.5 and 15 U/mL (or 0.1 and 1.0 μg/mL) and reaching a plateau in the reaction rate, thereafter indicating saturation of the reaction velocity (Figure 6). Because the canonical sequence DEVD is recognized by both Caspase-3 and -7 (7−10), our novel synthetic peptide substrate was hydrolyzed by both enzymes (see below for the data on Caspase-7). These reactions were demonstrated by two different investigators working in two separate laboratories located several miles apart. This showed the reproducibility, repeatability, and robustness of the assay.

We next investigated the reaction kinetics by conducting a time course of Caspase-3 hydrolysis of the DEVD−cyanine **3**. The results are presented in Figure 7 and show that the novel substrate was utilized rapidly and efficiently by Caspase-3. Hydrolysis of the DEVD−cyanine substrate was evident within 2 min of mixing of the enzyme at a concentration of 0.2 μg/mL with 250 μM substrate and incubating at 37 °C (Figure 7). These results are reminiscent of our earlier study with Caspase-3 enzyme (10). Saturation of the reaction was progressively reached between 20 and 90 min of reaction. The purpose of the experimental results described in Figures 6 and 7 was to establish the initial reaction rate conditions wherein substrate depletion does not take place. Such conditions will enable us to determine the affinity constant for the DEVD−cyanine **3** substrate for the Caspase-3 enzyme (described below).

A rectangular hyperbola type of tracing was obtained when increasing concentrations of the DEVD−cyanine **3** substrate were titrated into reaction wells containing a constant amount of enzyme (10 U/mL) (Figure 8A,B). This type of chart indicated that the classical Michaelis−Menten type of enzyme kinetics was operating during hydrolysis of the substrate by Caspase-3. There was a progressive increase in both blank-corrected fluorescence (Figure 8A) and S/B (Figure 8B) between DEVD−cyanine **3** concentrations of 10 and 250 μM. The Caspase-3 catalysis was saturated at concentrations greater than 250 μM. We utilized the Eadie−Hofstee transformation of these data to obtain an affinity constant of the substrate for the enzyme, a Km value of 22.7 ± 2.6 μM DEVD−cyanine **3**. This value is similar to the micromolar Km values reported in the literature using substrates that contained the same canonical DEVD tetrapeptide sequence but different reporter molecules such as coumarin derivatives (fluorescent assays) or *p*-nitro derivatives (colorimetric assays) (15−21). This observation suggested that the catalytic behavior of the Caspase-3 enzyme was not significantly altered due to the cyanine reporter group in our substrate relative to the chromogenic or fluorogenic reporter molecules tethered to the DEVD sequence in these earlier reports. We therefore used the 250 μM DEVD−cyanine **3** concentration routinely in our experiments, this value being 10-fold greater than Km and assured of substrate excess in order to maintain first-order reaction rate conditions.

We next focused our attention upon further assay optimization by determining the concentration of the carbohydrate scaffolds CMA and CMC necessary to generate maximal fluorescence following supramolecular self-assembly of the cyanine released from the DEVD−cyanine **3** covalent

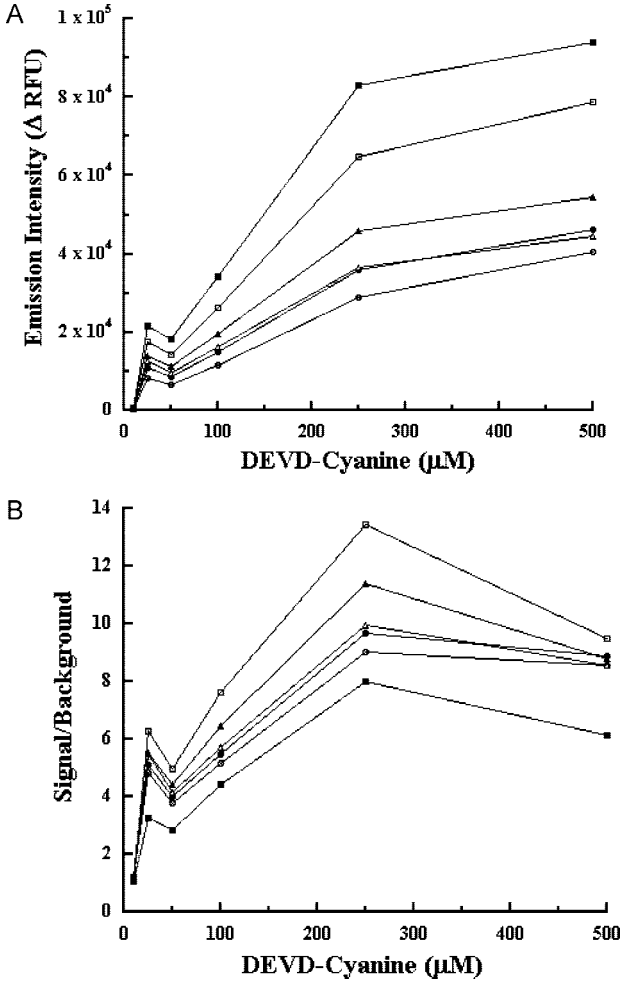

FIGURE 8. (A) DEVD−cyanine substrate dose−response curve. Increasing and indicated concentrations of the DEVD−cyanine substrate was reacted in the presence and absence of Caspase-3 under conditions described in the legends of Figures 6 and 7. A substrate concentration-dependent increase in the fluorescence emission intensity was observed up to 250 μM DEVD−cyanine, followed by a plateau at 500 μM substrate. The reaction samples were monitored for emission at 470 nm following excitation at the several different wavelengths of 420 nm (open circles), 425 nm (closed circles), 430 nm (open triangles), 435 nm (closed triangles), 440 nm (open squares), and 445 nm (closed squares). It is seen that the fluorescence emission intensity increases as the excitation wavelength increased from 420 to 445 nm. (B) Effect of the DEVD−cyanine concentration upon S/B. All reaction conditions were as described in the legend of part A. Unlike the fluorescence emission intensity (Figure 8A), the S/B increased with increasing excitation wavelength only up to 440 nm. The S/B at 445 nm was sharply lower relative to the S/B values observed at the other excitation wavelengths.

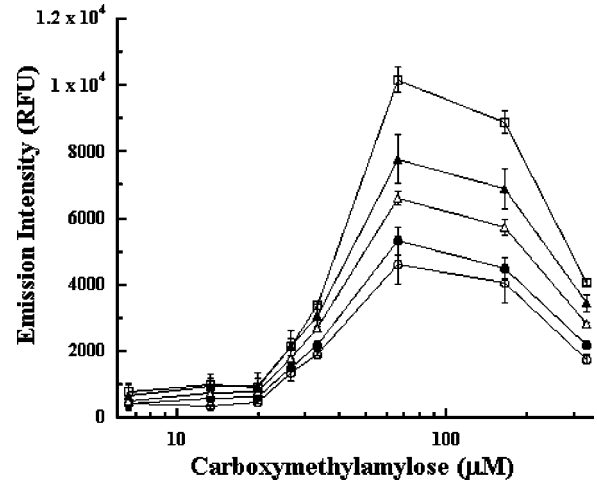

FIGURE 9. Optimization of the CMA scaffold. Increasing and indicated concentrations of the CMA scaffold were added to 0.2 μg/mL Caspase-3-catalyzed reactions carried out at 37 °C for 30 min. The fluorescence emission was monitored at 470 nm following excitation of the samples at 420 nm (open circles), 425 nm (closed circles), 430 nm (open triangles), 435 nm (closed triangles), and 440 nm (open squares).

adduct through Caspase-3 catalysis. The results showed that a minimum concentration of approximately 20 μM CMA was necessary to detect fluorescence (Figure 9). The fluorescence intensity increased linearly between 25 and 70 μM CMA followed by a decline between 150 and 300 μM CMA (Figure 9). The reasons for the decline in fluorescence emission at high concentrations of the scaffold were documented by us previously and included perturbations to the J aggregate and "inner filter" effects (4−6). We next fixed the CMA scaffold concentration at 65 μM and executed a titration experiment with increasing concentrations of CMC. The data showed that approximately 40 μM CMC resulted in a 3-fold increase in fluorescence over 65 μM CMA alone. On the basis of these results, we used a combination of 65 μM CMA and 35 μM CMC to effect scaffolding. We thus formulated a 1:1 mixture of 2 mM CMA and 1 mM CMC for addition to the reaction wells as described under the Materials and Methods section of the paper. By combining the twin scaffolds into a single solution, we also eliminated one operational step in the reaction protocol and simplified the assay conditions.

Fluorescence was detected immediately (less than 1 min) after the addition of the CMA + CMC scaffolds to the reaction wells. A 2-fold or greater increase in fluorescence resulted when the entire reaction mixture (postaddition of the scaffolds) was allowed to incubate at room temperature (~25 °C) for 30 min before taking fluorescence measurements (Figure 10). This suggested a time dependence to the self-assembly process of cyanine upon the carbohydrate scaffolds, hinting at the self-assembly kinetics as well as the stability of the self-assembled ensemble. Thus, the self-assembly kinetics of the cyanine upon the carbohydrate scaffolds of CMC and CMA are also reminiscent of the self-assembly of the same cyanine upon various nucleic acid scaffolds of DNA and RNA as reported by us recently (6). Depending upon the end-user requirements, the overall assay may be configured for either speed (2 min Caspase-3 catalysis as seen in Figure 7 and measurement of the fluorescence emission intensity "immediately") or for greater sensitivity (by waiting 30 min postaddition of the scaffolds mixture before taking fluorescence measurements).

Finally, we executed the Caspase-7 assay using the DEVD−cyanine substrate in 384-well plates for documenting the activity of this enzyme toward our novel peptide−cyanine substrate and for qualifying our assay to the HTS format appellation. The results are presented in Figure 11. Caspase-7 also utilized DEVD−cyanine as a substrate because it too recognized the canonical DEVD tetrapeptide sequence. Similar to Caspase-3 reaction kinetics (Figure 7),

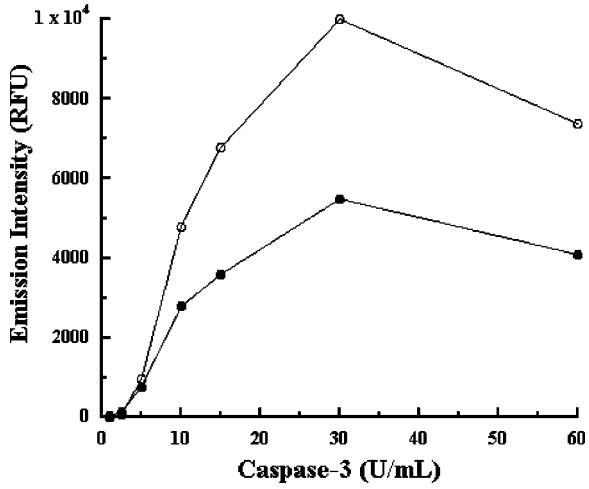

FIGURE 10. Self-assembly kinetics. Increasing and indicated concentrations of the Caspase-3 enzyme was reacted with a 50 μM DEVD−cyanine substrate at 37 °C for 2 h. Fluorescence emission was detected immediately after the addition of the CMA + CMC scaffolds mixture (closed circles) or 30 min postaddition of the scaffolds (open circles). All other conditions were as described in the Materials and Methods section of the paper.

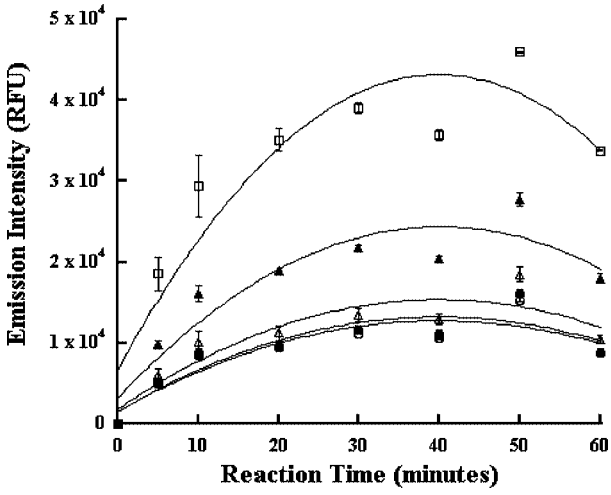

FIGURE 11. Caspase-7 HTS assay format. In this experiment, 2 μg/mL of Caspase-7 was reacted with 500 μM DEVD−cyanine in an assay buffer at 37 °C for the indicated reaction periods. Caspase-7 catalysis was stopped at the various time intervals by diluting the reaction well volume to 95 μL using a methanol/water mixture. At the end of 60 min, the CMA and CMC scaffolds mixture was added to the wells, followed by fluorescence measurements. The reaction samples were monitored for fluorescence emission at 470 nm following excitation at 420 nm (open circles), 425 nm (closed circles), 430 nm (open triangles), 435 nm (closed triangles), and 440 nm (open squares). The data were fitted using a polynomial (second-order) curve fit using *Kaleidagraph* software.

the Caspase-7 reaction proceeded linearly up to 20 min and began to plateau thereafter. The data scatter observed in Figure 11 required a polynomial (second-order) curve fit using *Kaleidagraph*, unlike the interpolative tracings of Figure 7. We attribute the data scatter to manual pipetting operations with the tiny wells of a 384-well microplate. Such scatter might be eliminated through robotic liquid handling, enabling more precise reagent dispensing and mixing that is a routine practice in high-throughput industrial laboratories (13). It must be noted that we have not yet optimized the protease assay completely in the 384-well plate format with either Caspase-3 or -7. Such optimization will also involve a thorough characterization of Caspase-7 kinetic parameters with the DEVD−cyanine substrate (for example, Km).

In conclusion, we demonstrated the utility of supramolecular self-assembly processes to generate a new class of enzyme substrates. Potentially, our substrate may be used to detect intracellular Caspase-3 and -7 activities because the cyanine also self-assembled upon nucleic acid scaffolds of DNA and RNA (6) in addition to the carbohydrate scaffolds (present data; also refs 1, 3, and 5). In this respect, our substrate is at the same time similar and different from the thiazole orange derivative of a DNA intercalating dye that was coupled to DEVD as a substrate for caspases (22). We are aware that the cyanine J-aggregate fluorescence is sensitive to environmental milieu (6, 23) and that the toxicity (cytotoxicity and antiproliferative activities) or the lack thereof of the cyanines (24, 25) will influence any utilities involving intracellular events tracking. These studies will be the focus of our future efforts with DEVD−cyanine.

The cyanine dye offers the prospect of self-assembly upon a broad range of scaffolds including CMA, CMC, HA, and single- and double-stranded, linear, or circular DNA and RNA (1, 3−6). Future studies will also involve the coupling of other signaling molecules in addition to cyanine as well as the exploration of other types of organic and inorganic scaffolds (such as proteins and clay nanoparticles) for the sensitive detection of a wide range of biochemical analytes. We plan to use our novel scaffold formation, disruption, destruction, or dye release enzymatic assays in a HTS format for the multiplexed, in vitro detection of a broad range of chemical−biological analytes.

Acknowledgment. Sandia National Laboratories is a multiprogram laboratory operated by Sandia Corp., a Lockheed Martin Company, for the United States Department of Energy under Contract DE-AC04-94AL85000. K.E.A. thanks the Defense Threat Reduction Agency-Joint Science and Technology Office (DTRA-JSTO; Contract AA07CBT008) for funding these investigations. The authors thank Dr. Satendra Chauhan, Director, Bachem BioScience, for valuable discussions regarding the covalent coupling of the DEVD tetrapeptide to cyanine. We acknowledge The University of New Mexico Mass Spectrometry facility for carrying out the mass spectrometry analyses described in this paper.

REFERENCES AND NOTES

(1) Kim, O.-K.; Je, J.; Jernigan, G.; Buckley, L.; Whitten, D. *J. Am. Chem. Soc.* **2006**, *128*, 510–516.
(2) Kobayashi, T. *J-Aggregates*; World Scientific Publishing Company: Singapore, 1996; p 228.
(3) Whitten, D. G.; Achyuthan, K. E.; Lopez, G. P.; Kim, O.-K. *Pure Appl. Chem.* **2006**, *78*, 2313–2323.
(4) Ogawa, K.; Achyuthan, K. E.; Chemburu, S.; Ji, E.; Liu, Y.; Lopez, G. P.; Schanze, K. S.; Whitten, D. G. In *Organic Semiconductors in Sensor Applications*; Bernards, D. A., Owens, R. M., Malliaras, G. G., Eds.; Springer-Verlag, Berlin, 2008; Vol. 107, pp 39−60.
(5) Achyuthan, K. E.; Lu, L.; Lopez, G. P.; Whitten, D. G. *Photochem. Photobiol. Sci.* **2006**, *5*, 931–937.
(6) Achyuthan, K. E.; McClain, J. M.; Zhou, Z.; Whitten, D. G.; Branch, D. W. *Anal. Sci.* **2009**, in press.
(7) Salvesen, G. S.; Riedl, S. J. *Adv. Exp. Med. Biol.* **2008**, *615*, 13–23.

(8) Earnshaw, W. C.; Martins, L. M.; Kaufman, S. H. *Annu. Rev. Biochem.* **1999**, *68*, 383–424.
(9) Talanian, R. V.; Quinlan, C.; Trautz, S.; Hackett, M. C.; Mankovich, J. A.; Banach, D.; Ghayur, T.; Brady, K. D.; Wong, W. W. *J. Biol. Chem.* **1997**, *272*, 9677–9682.
(10) Kumaraswamy, S.; Bergstedt, T.; Shi, X.; Rininsland, F.; Kushon, S.; Xia, W.; Ley, K.; Achyuthan, K.; McBranch, D.; Whitten, D. *Proc. Natl. Acad. Sci.* **2004**, *101*, 7511–7515.
(11) Meek, T. D.; Dreyer, G. B. *Ann. N.Y. Acad. Sci.* **1990**, *616*, 41–53.
(12) Eriks, J. C.; van der Goot, H.; Stark, G. J.; Timmerman, H. *J. Med. Chem.* **1992**, *35*, 3239–3246.
(13) Achyuthan, K. E.; Whitten, D. G. *Comb. Chem. HTS* **2007**, *10*, 399–412.
(14) Achyuthan, K. E. *Luminescence* **2001**, *16*, 257–262.
(15) Lien, S.; Pastor, R.; Sutherlin, D.; Lowman, H. B. *Protein J.* **2004**, *23*, 413–425.
(16) Stennicke, H. R.; Renatus, M.; Meldal, M.; Salvesen, G. S. *Biochem. J.* **2000**, *350*, 563–568.
(17) Nicholson, D. W.; Ali, A.; Thornberry, N. A.; Vaillancourt, J. P.; Ding, C. K.; Gallant, M.; Gareau, Y.; Griffin, P. R.; Labelle, M.; Lazebnik, Y. A.; Munday, N. A.; Raju, S. M.; Smulson, M. E.; Yamin, T.-T.; Yu, V. L.; Miller, D. K. *Nature* **1995**, *376*, 37–43.
(18) Gu, G.; Chumanevich, A. A.; Agniswamy, J.; Fang, B.; Harrison, R. W.; Weber, I. T. *Apoptosis* **2008**, *13*, 1291–1302.
(19) Lozanov, V.; Ivanov, I. P.; Benkova, B.; Mitev, V. *Amino Acids* **2008**, July 3, DOI 10.1007/s00726-008-0136-4, Epub ahead of print.
(20) Stennicke, H. R.; Salvesen, G. S. *Cell Death Differ.* **1999**, *6*, 1054–1059.
(21) Takahashi, T.; Ogo, M.; Hibino, T. *J. Invest. Dermatol.* **1998**, *111*, 367–372.
(22) Cen, H.; Mao, F.; Aronchik, I.; Fuentes, R. J.; Firestone, G. L. *FASEB J.* **2008**, *22*, 2243–2252.
(23) Wang, M.; Silva, G. L.; Armitage, B. A. *J. Am. Chem. Soc.* **2000**, *122*, 9977–9986.
(24) Delaey, E.; van Laar, F.; De Vos, D.; Kamuhabwa, A.; Jacobs, P.; de Witte, P. *J. Photochem. Photobiol. B* **2000**, *55*, 27–36.
(25) Sima, P. D.; Kanofsky, J. R. *Photochem. Photobiol.* **2000**, *71*, 413–421.

AM800091H